Soil Response and Modeling of Soft Soil Subgrades under Cyclic Rail Loading

Buddhima Indraratna, Ph.D., F.ASCE, [1] Bin-Hua Xu, Ph.D., [2] and Cholachat Rujikiatkamjorn, Ph.D., M.ASCE[3]

[1]Transport Research Centre, School of Civil and Environmental Engineering, University of Technology Sydney, NSW 2007, Australia; E-mail: buddhima.indraratna@uts.edu.au
[2]Transport Research Centre, School of Civil and Environmental Engineering, University of Technology Sydney, NSW 2007, Australia; E-mail: binhua.xu@uts.edu.au
[3]Transport Research Centre, School of Civil and Environmental Engineering, University of Technology Sydney, NSW 2007, Australia; E-mail: cholachat.rujikiatkamjorn@uts.edu.au

ABSTRACT

Soft soil is prevalent worldwide, especially in coastal regions, making it crucial to thoroughly understand its behaviour under cyclic loading to ensure the proper design of railway substructures. The operation of heavy freight trains induces a notable increase in excess pore water pressure (EPWP) and plastic strain, if not adequately dissipated or drained, which can temporarily reduce the bearing capacity, potentially leading to severe damage to rail infrastructure such as mud pumping, ballast degradation, and excessive settlement. This research delves into the behaviour of soft soils under undrained cyclic loading, with different cyclic stress ratios (CSR), through a series of cyclic tests. The Modified Cam Clay (MCC) model, is extended to predict soil response under undrained cyclic loading by incorporating a dynamic yield surface during cyclic loading. Results reveal that beyond a critical cyclic stress ratio (CSRc), both EPWP and axial strain experience a rapid escalation after a certain number of cycles. Moisture and fine particles migrate upwards toward the specimen's top, contributing to soil softening and fluidization and leading to soil instability. The findings highlight the significant impact of drainage conditions via geosynthetics on soft soil subgrade stability under cyclic loads. The installation of vertical drains is shown to enhance radial drainage, facilitating the dissipation of EPWP, thereby enhancing soil stability. Geosynthetics are proven effective in mitigating fine particle migration and EPWP accumulation, thereby reducing the EPWP gradient and preventing mud pumping.

INTRODUCTION

The resilience and stability of railway substructures are paramount for ensuring safe and efficient railway operations (Indraratna et al. 2011; Lazorenko et al. 2020). Soft subgrade soils, particularly low plasticity clays, which are prevalent in coastal regions worldwide, pose significant challenges for the design and maintenance of railways due to their susceptibility to deformation and instability under cyclic loading conditions (Indraratna et al. 2021; Xu et al. 2020, 2022). Previous studies revealed that heavy freight trains induce significant excess pore water pressure (EPWP) and plastic strain in soft subgrades (Bian et al. 2019). This can result in subgrade fluidization, mud pumping, ballast degradation, and excessive subsidence, highlighting the necessity of thoroughly

understanding the cyclic behaviour of soft soils to develop effective mitigation strategies. (Indraratna et al. 2020b; Nguyen et al. 2019).

This study investigates the behaviour of soft subgrade soils under undrained cyclic loading, integrating theoretical and experimental insights to capture the influence of drainage provided by geosynthetics. The objective is to improve railway engineering practices by advancing the understanding of soft soil behaviour under cyclic loading and proposing practical strategies for the resilient design and maintenance of railway substructures.

UNDRAINED CYCLIC RESPONSE OF SOFT SOIL SUBGRADES

Experimental investigation

Testing materials and cyclic triaxial test program

To investigate the undrained cyclic response of soft soil samples (LL= 26%, w =14.6%) were collected from a field site near Wollongong, NSW, Australia, which is known for its history of mud pumping. The soil was classified as a low-plastic clay (CL) with a plasticity index of about 11, according to ASTM standard D2487-17 (ASTM standard D2487-17 2017). The natural subgrade soil samples were reconstituted to produce test specimens with varying compacted dry densities (1600-1790 kg/m³) and kaolin contents (0-30%). Different frequencies and cyclic stress ratios (CSR) were also applied, where CSR is defined as the ratio of applied deviator stress (σ_d) to twice the confining pressure (σ_c), i.e., CSR = σ_d /(2 × σ_c), using cyclic triaxial apparatus where the test program is detailed in Table 1. The tested frequency range (1.0– 5.0 Hz) was applied which corresponds to train speeds of approximately 45–225 km/h. As the in situ subgrade stresses are anisotropic, a ratio of horizontal to vertical stress of 0.6 was determined for the tested soil. The remoulded specimens, measuring 50 mm in diameter and 100 mm in height, were prepared using moist tamping to minimize particle segregation. Additionally, the nonlinear under-compaction criterion proposed by Jiang et al. (2003) was employed to achieve uniform-density test specimens, ensuring repeatability in the tests. Saturation was carried out by de-airing the sample and filling the cell with filtered and de-aired water until a Skempton's B-value exceeded 0.95.

Table 1. Cyclic triaxial test program.

Soil type	ρ_d (kg/m^3)	e_0	CSR	f (Hz)	σ_d (kPa)	σ_c (kPa)
Original soil	1600	0.644	0.1-0.4	1, 2, 5	10	15
	1680	0.556	0.2-0.5			
	1790	0.469	0.2-1.0			
Original soil	1620	0.640	0.3	5	13.3	20
Original soil +10 % Kaolin		0.620				
Original soil +30 % Kaolin		0.610				

Testing results and discussion

(1) Cyclic stress ratio (CSR): Typical variations of permanent axial strain (ε_a) for the specimen with a dry density (ρ_d) of 1790 kg/m³ subjected to a frequency of 1.0 Hz. under different CSRs are shown in Fig. 1a. When CSR < 0.5, the cyclic axial strain (ε_a) gradually stabilizes as the number of cycles

(N) increases; for example, ε_a stabilizes at 0.6% after 1000 cycles. However, when CSR ≥ 0.5, ε_a increases rapidly, indicating early soil instability. For example, at CSR = 0.5, ε_a jumps from 0.5% at N = 10 to 2.6% at N = 50, with a critical number of cycles, $Nc \approx 32$, before stabilizing at ε_a = 5% after $N > 50$.

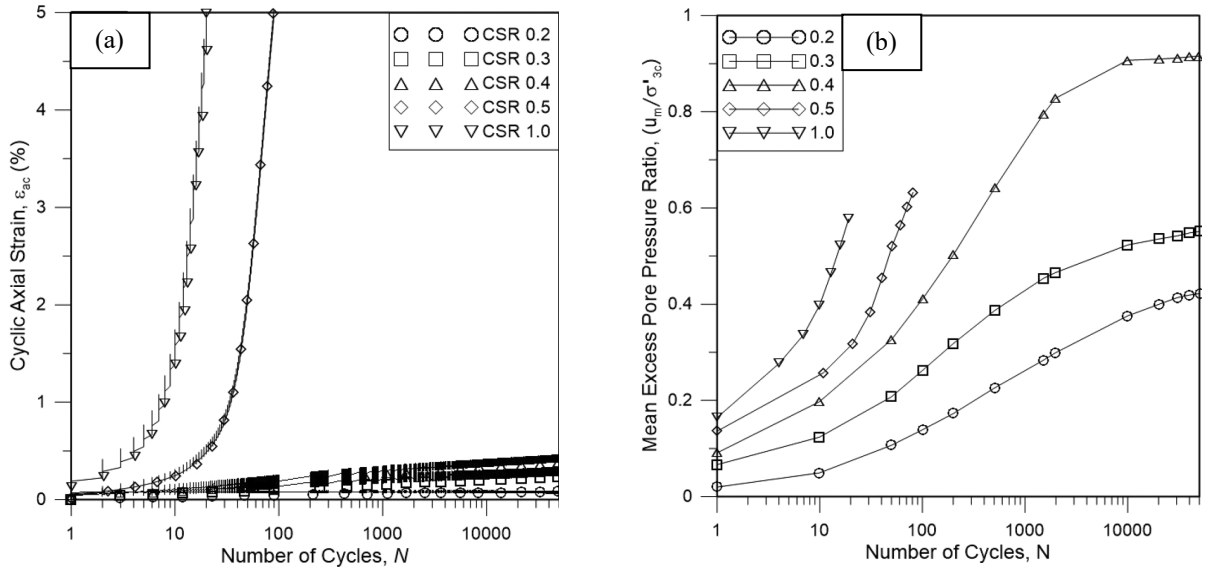

Figure 1. Development of (a) cyclic axial strain and (b) mean excess pore pressure ratio (ρ_d = 1790 kg/m3; f = 1.0 Hz). (with permission, Indraratna et al. 2020b)

As CSR increases, excess pore pressure (EPP) also rises (Fig. 1b), with the rate of increase varying due to CSRs. A critical CSR (CSRc) exists where EPP rapidly increases, marking an unstable state where the soil becomes slurry. This deformation is accompanied by a drop in deviatoric stress in the stress path when CSR ≥ 0.5, indicating a loss of shear strength due to fluidization before reaching the conventional undrained failure line. In contrast, for stable specimens (CSR < CSRc), the stress path remains below the failure envelope.

(2) Frequency (f): Figure 2a illustrates the effect of frequency on the development of cyclic axial strains. For CSR < CSRc, where the samples do not fluidize, higher frequencies result in more significant cyclic axial strains. For example, at f = 1.0 Hz, ε_a gradually increases to 0.25% at N = 50,000 cycles, whereas at f = 5.0 Hz, ε_a reaches 0.9% at the same N. This cyclic axial strain includes both recoverable and residual components, accumulating over many cycles under undrained cyclic load. For CSR = 0.5, above the critical value CSRc, higher frequencies delay the onset of soil fluidization. For instance, the rapid growth of EPP and residual axial strain (ε_a) occurs at $N \approx 32$ cycles (t = 20 s) for f = 1.0 Hz, but takes nearly 3200 cycles (t = 240 s) at f = 5.0 Hz. Lower frequencies imply a longer loading period before unloading, leading to larger residual EPP and axial strain. These observations suggest that lower frequencies can sometimes initiate fluidization earlier when CSR > CSRc.

(3) Dry density: Figure 2b shows the effect of dry density on the undrained cyclic response of subgrade soil. Samples with higher dry density or relative compaction better resist cyclic loads under the same conditions, resulting in a higher threshold for the critical stress ratio (CSRc) (Fig. 2b). For instance, samples with ρ_d = 1790 kg/m³ fluidize at CSR ≥ 0.5, whereas lower density samples (1600

and 1680 kg/m³) fluidize at lower CSRs. Although lower density specimens fail at smaller CSRs, it takes more cycles to initiate fluidization at the corresponding CSRc.

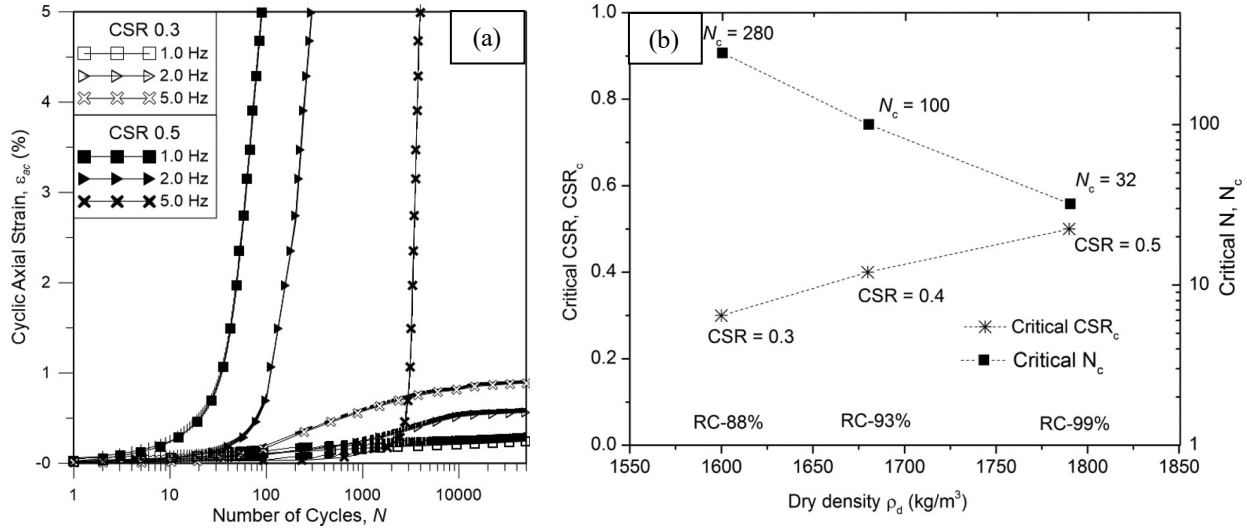

Figure 2. Effects of (a) loading frequency and (b) dry density. (with permission, Indraratna et al. 2020b)

(4) Kaolin content: As Figure 3 shows, increasing Kaolin content enhances the shearing resistance to cyclic loading, as evidenced by increasing the critical number of cycles within a stabilized stress path. Figure 3a compares the cyclic stress paths of specimens with additional Kaolin contents of 0% (K0), 10% (K10), and 30% (K30) with the same dry density (1620 kg/m³) and the same loading conditions (CSR = 0.3, f = 5 Hz). K0 specimen softens after about 39 cycles, while K10 specimen maintains constant deviator stress (q) with p' stabilizing before undrained shear failure after 135 cycles. Specimen K30 shows similar behaviour with less reduction in p'.

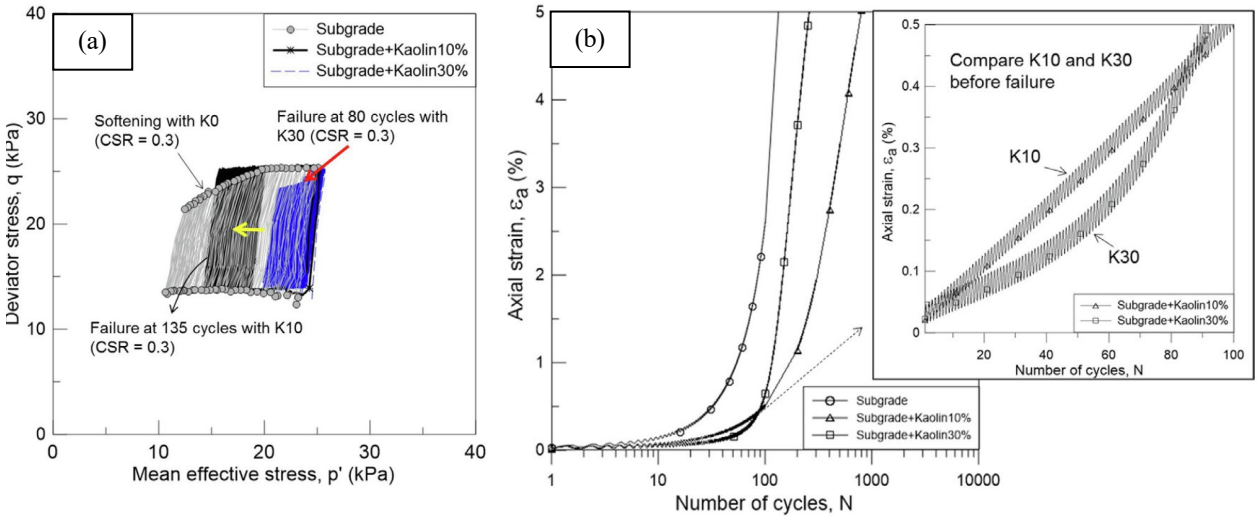

Figure 3. Influence of Kaolin content on the cyclic response of subgrade soil (ρ_d = 1620 kg/m3): (a) stress paths and (b) axial strains. (with permission, Indraratna et al. 2020a)

Figure 3b shows that all specimens experience a rapid increase in ε_a, indicating failure at CSR = 0.3. K0 specimen shows a sharp strain increase after 39 cycles, while a similar beahviour can be

observed for K10 specimen after 135 cycles. Additional Kaolin reduces ε_a development, allowing more cycles before failure. However, increasing Kaolin to 30% decreases cyclic resistance, with N_c dropping to about 80, suggesting an optimal Kaolin content between 10% and 30%. Thus, soils with higher PI are not easy to fluidization or mud pumping, which indicates that adding reasonable amount of cohesive fines can enhance the resistance of subgrade soil that is prone to fluidization.

Theoretical development

Theoretical background

The Modified Cam Clay (MCC) model has been incorporated into two theoretical models to predict soil behaviour under cyclic loading (Ni et al. 2015; Truong et al. 2021). Some fundamental theoretical backgrounds are summarised below. The mean effective stress p', deviator stress q, and stress ratio are defined as $p' = \left(\sigma_1' + 2\sigma_3'\right)/3$, $q = \sigma_1 - \sigma_3$ and $\eta = q/p'$, where σ_1' and σ_3' are the effective major and minor principal stress, respectively. The corresponding incremental volumetric strain $d\varepsilon_v$ and shear strain $d\varepsilon_s$ can be divided into elastic and plastic components which are calculated by $d\varepsilon_v = d\varepsilon_v^e + d\varepsilon_v^p$ and $d\varepsilon_s = d\varepsilon_s^e + d\varepsilon_s^p$.

Elastic strains

Based on the MCC model, the volumetric and shear components of elastic strain are given by $d\varepsilon_v^e = \kappa\, dp'/vp'$ and $d\varepsilon_s^e = dq/3G$, where v is the specific volume, which is equal to 1+e_0; κ is the slope of swelling lines in $v - \ln p'$ space; and G is the shear modulus.

Yield surface models for cyclic loading

This section explores two hypotheses that modify the Modified Cam Clay (MCC) yield surface to simulate soil behaviour under cyclic loading. In the first hypothesis, the yield surface changes in size but retains its shape during each unloading path. In contrast, the second hypothesis assumes that the yield surface changes in shape while maintaining a constant size, with p_c' remaining constant during unloading. Here, unloading is defined as an initial reduction in the magnitude of the deviator stress. The first approach is inspired by the seminal work of Carter et al. (1982) and was successfully extended in later studies (Ni et al. 2015; Wang et al. 2019). The second approach based on McDowell and Hau (2004), was extended with success in subsequent research (Truong et al. 2021). Detailed descriptions of the yield surface models and processes in Models A and B are provided below.

(1) Model A: The size of the yield surface shrinks during unloading

Ni et al. (2015) proposed an undrained cyclic loading model based on the framework of the modified Cam-Clay model. A parameter θ^* was introduced to express the rate that the yield surface shrinks its size over the number of cycles. The Hardening parameter can be governed by:

$$\frac{dp_c'}{p_c'} = \theta^* \frac{dp_y'}{p_y'} = \frac{1}{\xi_1 N + \xi_2} \frac{dp_y'}{p_y'} \tag{1}$$

where ξ_1 and ξ_2 are cyclic degradation parameters, p_y' is a variable defined by:

$$p'_y = p' + \left(\frac{q}{M}\right)^2 \frac{1}{p'} \tag{2}$$

The variation in the stress path under cyclic loading based on Model A is illustrated in Fig. 4a.

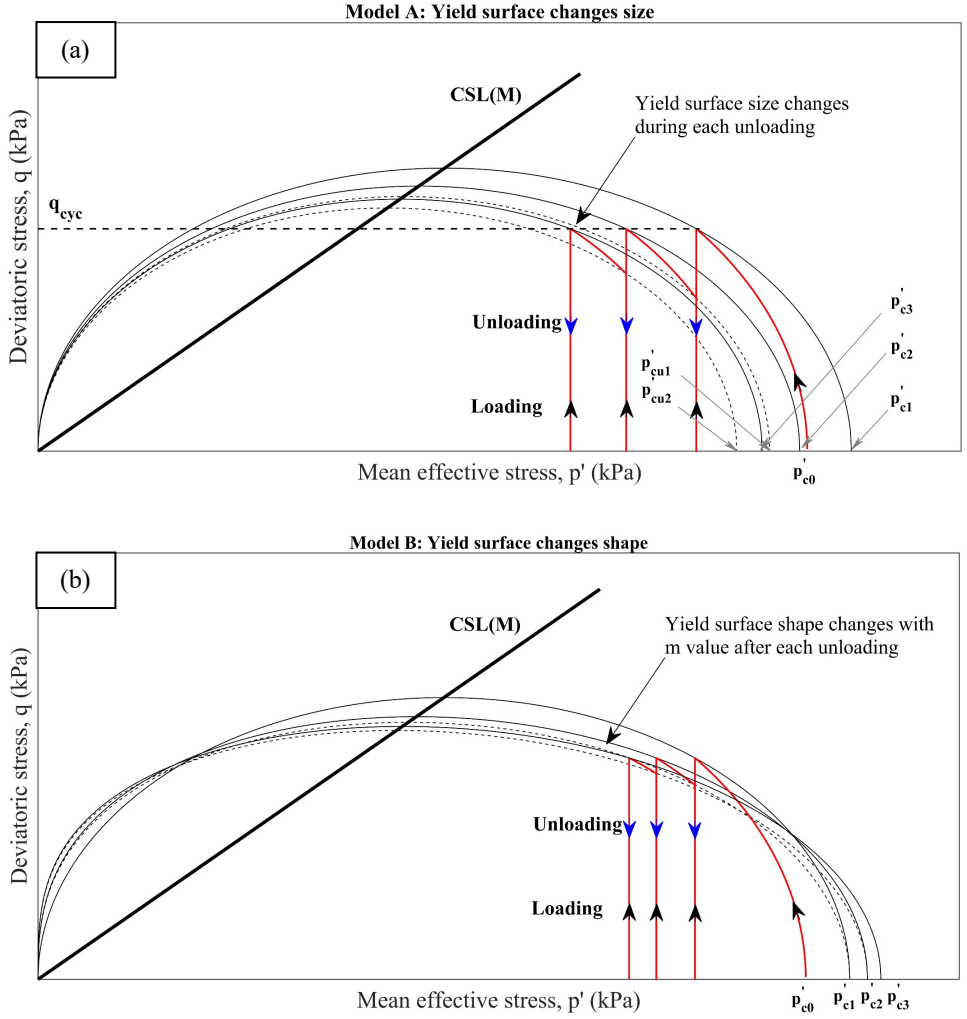

Figure 4. Stress path under cyclic loading (a) Model A and (b) Model B.

(2) Model B: The shape of the yield surface changes during cyclic loading

McDowell and Hau (2004) proposed the generalised MCC model to consider the soil properties and the initial loading conditions, as given by:

$$q^2 = \frac{M^2}{1-m} p'^2 \left[1 - \left(\frac{p'}{p'_c}\right)^{2\left(\frac{1-m}{m}\right)}\right] \tag{3}$$

where m is the parameter that defines the shape of the yield surface. Note that when m = 2, the conventional MCC model is recovered. Truong et al. (2021) proposed a concept the number of cycles yielding plastic strains, N_p, is incorporated into the function of m, as represented by the relationship $m = \frac{\alpha N_p^{0.5}}{N_p^{0.5} + \beta}$, where α and β are parameters that specify how cyclic loading distorts the yield surface.

The variation in the stress path under cyclic loading based on Model B is illustrated in Fig. 4b.

Flow rules, plastic potential, and hardening rule

In Model A, the associated flow rule is used, which is the same as the MCC model, where the plastic potential is identical to the yield surface. In contrast, Model B employs a non-associated flow rule, where the plastic potential is governed independently from the yield surface. Specifically, a parameter m^* is introduced to replace the m in Eq. (3) as the additional parameter controlling the shape of plastic potential. The flow rule can then be given by $\frac{d\varepsilon_v^p}{d\varepsilon_s^p} = \frac{M^2 - \eta^2}{m^* \eta}$. For models A and B, a hardening model similar to the MCC model is used, which assumes a change of p_c' is only induced by a change of plastic volumetric strain, so that: $\frac{dp_c'}{d\varepsilon_v^p} = \frac{vp_c'}{\lambda - \kappa}$, where λ is the slope of normal compression lines in $v - \ln p'$ space.

Model applications and discussion

Figure 5 shows the predictions of Models A and B for experiment Series II on silty soil (Indraratna et al. 2020b). The parameters used in the application are summarised in Table 2 (Indraratna et al. 2021). For this low-plasticity soil (PI = 11), Model B provides more accurate predictions for both stable (CSR = 0.3) and unstable (CSR = 0.5) cases. Model B's EPWP estimates closely match experimental data up to 1500 cycles, while Model A significantly overestimates EPWP initially (N < 450). For unstable specimens, Model B better predicts the rapid EPWP increase and corresponding axial strain rise to 5% within the first 100 cycles.

Table 2. Properties of subgrade soil collected from mud pumping site after remediation.

κ	λ	M	ξ_1	ξ_2	α	β	CSR	f
0.1	0.05	1.89	8	200	40	190	0.3	1
			8	800	40	575	0.5	1

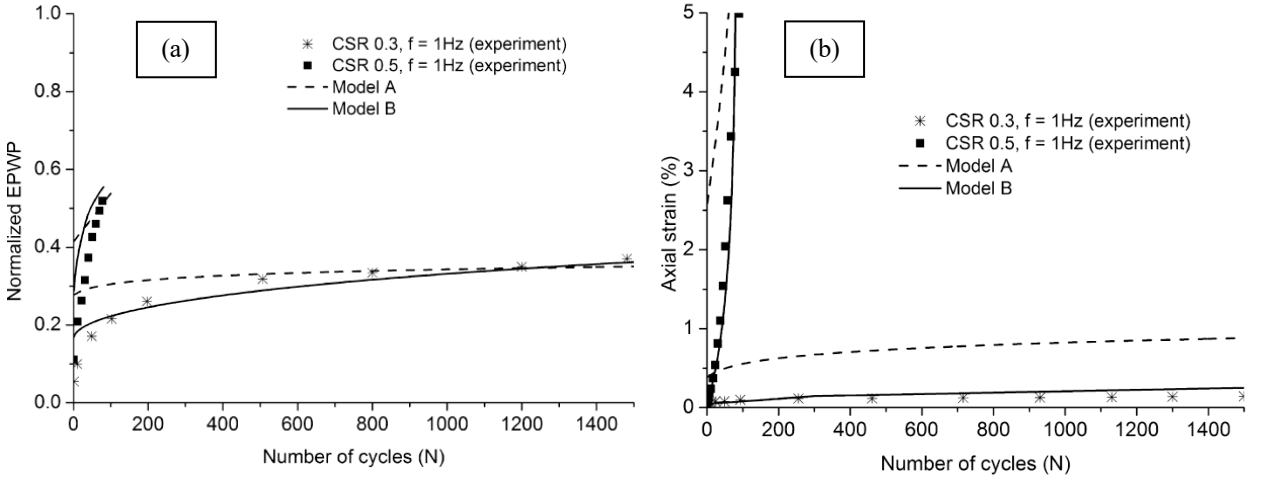

Figure 5. Predictions using Models A and B: a) EPWP and b) axial strain. (with permission, Indraratna et al. 2020b)

There is also a notable difference in cyclic behaviour between the two tested soils despite similar loading conditions. For f = 1 Hz and at critical CSRc, Kaolin clay soil (Series I, PI = 22) requires about 7500 cycles to trigger instability, whereas silty soil (Series II, PI = 11) becomes unstable after just over 30 cycles. Lower plasticity soils, like sandy to silty soils, become unstable earlier due to their lack of cohesive bonding, making them more susceptible to EPWP.

THE EFFECTIVENESS OF GEOSYNTHETICS IN MITIGATING INSTABILITY AND FLUIDIZATION

Based on the above experimental and theoretical analysis, the soft subgrade is prone to fluidization when it is under undrained cyclic loading conditions, especially for lower plasticity soils. To address these challenges, a series of cyclic tests were further conducted to assess the effectiveness of geosynthetics in mitigating instability and fluidization.

Table 3. Dynamic filtration tests program.

Test Name	U	P	G	P+G
Drainage condition	Undrained	With PVD	With geocomposites	With PVD+ geocomposites

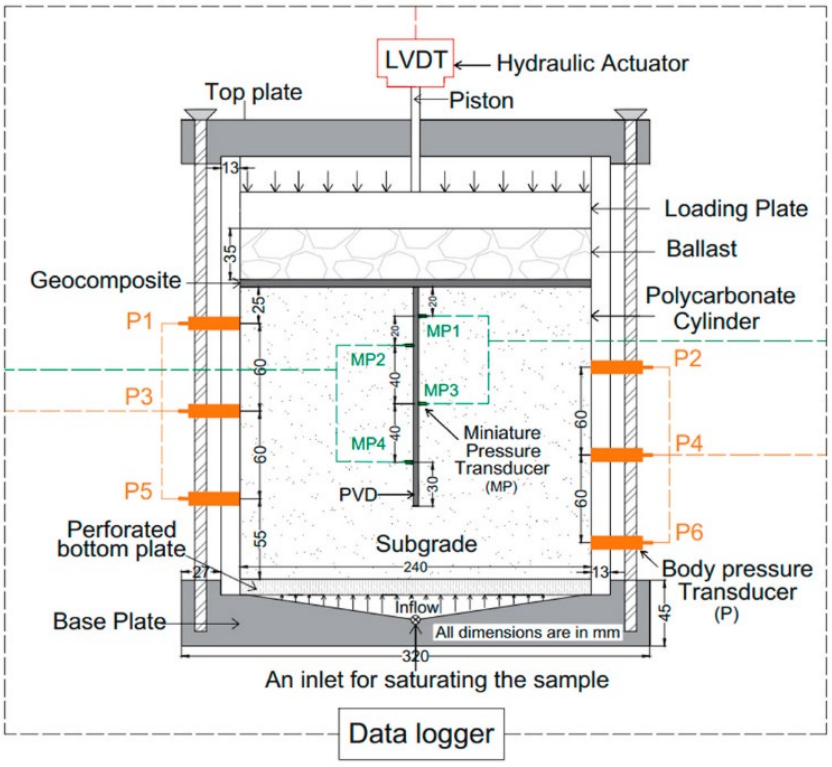

Figure 6. Schematic diagram of DFA. (with permission, Arivalagan et al. 2022)

The dynamic filtration apparatus (DFA) was used to conduct dynamic tests. The schematic diagram of the DFA with instrumentation is shown in Fig. 6. A total vertical pressure of 30 kPa was applied for 48 hours to consolidate the soil specimen. A uniform cyclic stress at a frequency of 5 Hz was applied as a minimum vertical stress, and the sinusoidal vertical cyclic stress (σ_{min} = 30 kPa and

σ_{max} = 70 kPa) simulates a maximum axle load of 35 tonnes. The entire test program of dynamic filtration tests that cover various ballast/subgrade interface conditions is summarised in Table 3. The geocomposite was placed on top of the specimen to enhance the drainage capacity at the subgrade/ballast interface. The prefabricated vertical drains (PVDs) used in this test were scaled down for the cyclic experiments to mimic field conditions where they were installed 1–1.5 m apart, so they could attain a similar time scale effect under a reduced drainage path. Based on a DFA diameter of 240 mm, the modified PVDs used for the laboratory experiments were 17 mm × 3.4 mm.

Figure 7a shows that the EPWP in Test P is significantly lower than in Test G from the start of the cyclic test. For instance, in Test G, EPWP at MP2 (40 mm) exceeds 37 kPa after 500 cycles, while in Test P it remains below 22 kPa. Test G could not dissipate EPWP below 15 kPa in the middle region until 30,000 cycles (1.67 hours), whereas Test P effectively dissipates EPWP at all depths, with EPWP at MP3 staying under 4 kPa after 75,000 cycles. Figure 7b demonstrates that the combined PVD and geocomposite system (P+G) reduces EPWP to less than 15 kPa within 500 cycles and below 4 kPa after 75,000 cycles. The undrained test (Test U) shows a maximum EPWP over 25 kPa at 75,000 cycles, but the PVD-geocomposite system reduces EPWP by approximately 88% at 80 mm depth. These results confirm that the PVD-geocomposite system effectively stabilizes subgrade soil under cyclic loading, mitigating mud pumping and enhancing foundation stability.

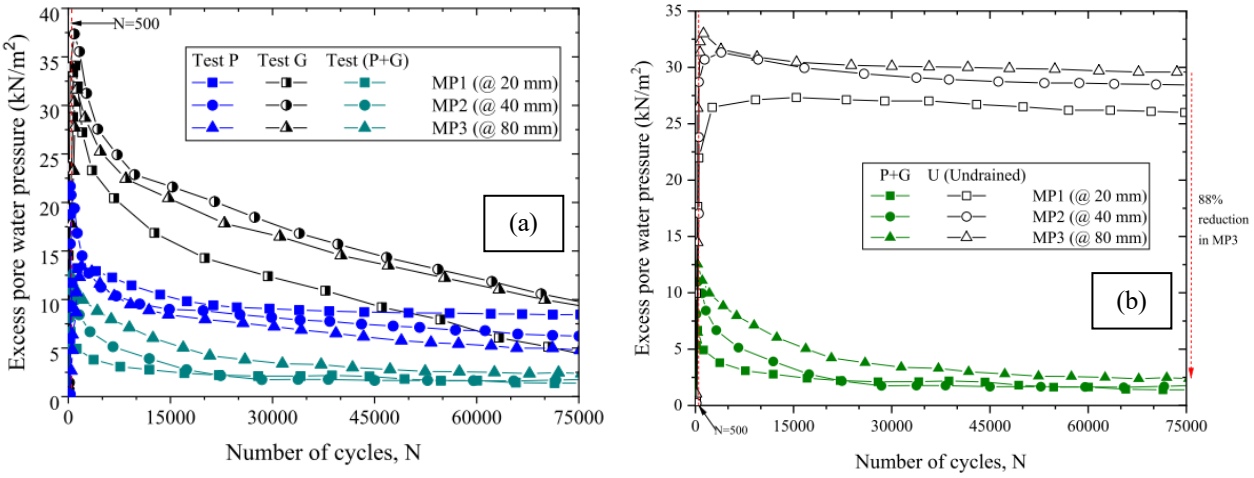

Figure 7. Development of EPWP. (with permission, Arivalagan et al. 2022)

CONCLUSION

This study provides a comprehensive investigation into the behaviour of soft subgrade soils under cyclic rail loading, the key findings include:

(1) Higher CSR and lower frequencies accelerate excess pore water pressure and cyclic axial strain, leading to failure. Higher dry density and optimal Kaolin content improve resistance.

(2) Theoretical models based on the MCC framework, especially Model B, can well predict the undrained cyclic behaviour of soft soil.

(3) Geosynthetics like PVDs (1–1.5 m apart) and geocomposites effectively reduce fluidization and improve soil stability for new railway construction.

ACKNOWLEDGEMENT

The Authors gratefully acknowledge the financial assistance from the Australian Research Council. A number of past research students of Prof. Indraratna, namely, Dr. Jing Ni, Dr Thanh Trung Nguyen, Dr. Mandeep Singh, Dr. Aruni Abeywickrama, Dr. Warantorn Korkitsuntornsan, Dr. Minh Hoang Truong and Dr. Joseph Arivalagan have also contributed to the contents of this paper through their research work. Much of the contents reported in this paper are described in detail in a number of scholarly journals including Canadian Geotechnical Journal, Computers and Geotechnics, Geotextiles and Geomembranes, Transportation Geotechnics and ASCE International Journal of Geomechanics among others, as cited in the text and listed below.

REFERENCES

Arivalagan, J., Indraratna, B., Rujikiatkamjorn, C., and Warwick, A. (2022). 'Effectiveness of a Geocomposite-PVD system in preventing subgrade instability and fluidisation under cyclic loading'. *Geotextiles and Geomembranes*, Elsevier Ltd, 50(4), 607–617.

ASTM standard D2487-17. (2017). *Standard practice for classification of soils for engineering purposes (unified soil classification system)*. *ASTM*, 1–12.

Bian, X., Hu, J., Thompson, D., and Powrie, W. (2019). 'Pore pressure generation in a poro-elastic soil under moving train loads'. *Soil Dynamics and Earthquake Engineering*, Elsevier Ltd, 125(December 2018), 105711.

Carter, J. P., Booker, J. R., and Wroth, C. P. (1982). *A critical state soil model for cyclic loading*. *Soil mechanics—Transient and cyclic loading*, (E. G.N. Pande, O. C. Zienkiewicz, ed.), Wiley, Chichester, U.K.

Indraratna, B., Korkitsuntornsan, W., and Nguyen, T. T. (2020a). 'Influence of Kaolin content on the cyclic loading response of railway subgrade'. *Transportation Geotechnics*, Elsevier, 22(August 2019), 100319.

Indraratna, B., Nguyen, T. T., Singh, M., Rujikiatkamjorn, C., Carter, J. P., Ni, J., and Truong, M. H. (2021). 'Cyclic loading response and associated yield criteria for soft railway subgrade – Theoretical and experimental perspectives'. *Computers and Geotechnics*, Elsevier Ltd, 138, 104366.

Indraratna, B., Salim, W., and Rujikiatkamjorn, C. (2011). *Advanced rail geotechnology - Ballasted track. CRC Press/Balkema*.

Indraratna, B., Singh, M., Nguyen, T. T., Leroueil, S., Abeywickrama, A., Kelly, R., and Neville, T. (2020b). 'Laboratory study on subgrade fluidization under undrained cyclic triaxial loading'. *Canadian Geotechnical Journal*, 57(11), 1767–1779.

Jiang, M. J., Konrad, J. M., and Leroueil, S. (2003). 'An efficient technique for generating homogeneous specimens for DEM studies'. *Computers and Geotechnics*, 30(7), 579–597.

Lazorenko, G., Kasprzhitskii, A., Kukharskii, A., Kochur, A., and Yavna, V. (2020). 'Failure analysis of widened railway embankment with different reinforcing measures under heavy axle loads: A comparative FEM study'. *Transportation Engineering*, Elsevier Ltd, 2, 100028.

McDowell, G. R., and Hau, K. W. (2004). 'A generalised Modified Cam clay model for clay and sand incorporating kinematic hardening and bounding surface plasticity'. *Granular Matter*, 6(1), 11–16.

Nguyen, T. T., Indraratna, B., Kelly, R., Phan, N. M., and Haryono, F. (2019). 'Mud pumping under railtracks: Mechanisms, assessments and solutions'. *Australian Geomechanics Journal*, 54(4), 59–80.

Ni, J., Indraratna, B., Geng, X.-Y., Carter, J. P., and Chen, Y.-L. (2015). 'Model of Soft Soils under Cyclic Loading'. *International Journal of Geomechanics*, 15(4), 04014067.

Truong, M. H., Indraratna, B., Nguyen, T. T., Carter, J., and Rujikiatkamjorn, C. (2021). 'Analysis of undrained cyclic response of saturated soils'. *Computers and Geotechnics*, Elsevier Ltd, 134(February), 104095.

Wang, Y., Lei, J., and Wang, Y. (2019). 'A post-cyclic strength degradation model for saturated soft clay'. *Ocean Engineering*, Elsevier Ltd, 186.

Xu, B.-H., He, N., Jiang, Y.-B., Zhou, Y.-Z., and Zhan, X.-J. (2020). 'Experimental study on the clogging effect of dredged fill surrounding the PVD under vacuum preloading'. *Geotextiles and Geomembranes*, 48(5), 614–624.

Xu, B.-H., Indraratna, B., Rujikiatkamjorn, C., and Nguyen, T. T. (2022). 'A large-strain radial consolidation model incorporating soil destructuration and isotache concept'. *Computers and Geotechnics*, Elsevier Ltd, 147, 104761.